

# Basic principle and operation methods of the direct-derivation method

Hideo Toraya\*

## 1. Introduction

Quantitative phase analysis (QPA) using the X-ray diffraction technique is routinely employed to find weight ratios of individual component phases in a mixture. Techniques for QPA have been widely used not only in research and development but also routinely deployed for quality control of industrial products. Various techniques have been proposed for QPA in past decades<sup>(1)</sup>. Some techniques are designed for exclusive use in QPA of specific materials such as zirconia<sup>(2)</sup>, silicon nitrides<sup>(3)</sup> *etc.*, while the calibration-curve method<sup>(4)</sup>, the reference intensity ratio (RIR) method<sup>(5),(6)</sup>, and the Rietveld method<sup>(2),(7)-(9)</sup> have been applied to QPA of general materials. The direct derivation method (DDM) is also a QPA technique suitable for use with general materials<sup>(10)-(15)</sup>. The observed diffraction pattern of a mixture is the superposition of component patterns for individual phases. In conducting QPA, the observed diffraction intensities of the mixture must be separated into intensity datasets of the individual components. In deriving the weight ratios from intensity datasets, the Rietveld method uses crystal structure parameters while the RIR method uses experimentally derived or calculated RIR. Unlike other methods, the DDM requires only chemical composition data of the individual components. Chemical composition data are available in almost all cases, since QPA is usually conducted after phase identification or applied to chemically known materials. Therefore, the DDM has no limitation in applying QPA to any materials as long as the intensity datasets for the individual components are available.

Basic principle of the DDM is very simple. Parameters, used for deriving the weight ratios, can definitely be calculated using chemical composition data. Therefore, its accuracy in QPA is mostly dependent on the accuracy in the intensity datasets for individual components. Thus the correct choice of a decomposition tool, for a given situation, will deliver the highest quality result. Therefore, it is important to understand handling of various techniques used for separating the observed pattern into the component patterns. Readers of this article may be engaged in various analytical works, with many of them having experiences with QPA. Some of them will also be interested in reading original articles. So core mathematical formulas are presented at each

step of this article. Theoretical and experimental details are located in references 10 to 15.

## 2. Basic principle of the DDM

Let us consider a solid cube as shown in Fig. 1. We would like to weigh the cube. The cube is, however, too big to be weighed with an analytical balance, while its volume ( $V_{\text{cube}}$ ) can easily be measured with a ruler. If we know the volume per unit weight ( $V_{1g}$ , or specific volume) for the material that constitutes the cube, then we can easily derive the weight of the cube ( $W_{\text{cube}}$ ) by

$$W_{\text{cube}} = \frac{V_{\text{cube}}}{V_{1g}} \quad (1)$$

The DDM is based on the same idea as that represented by equation (1): the volume of the cube can be replaced with the total sum of scattered intensities ( $S$ ) from the material irradiated by X-rays. We can derive the weight of the material by dividing the  $S$  by the scattered intensity per unit weight ( $S_{1g}$ ). In the case of a  $K$ -component mixture, the weight of the  $k$ th component ( $W_k$ ) can be calculated by

$$W_k = C \frac{S_k}{a_k^{-1}} = Ca_k S_k \quad (2)$$

where  $S_k$  is the total sum of scattered intensities ( $S$ ) for the  $k$ th component,  $a_k^{-1}$ , the reciprocal form of  $a_k$ , is the scattered intensity per unit weight ( $S_{1g}$ ), and  $C$  is the proportional constant. It is experimentally difficult to measure the scattered intensity on an absolute scale; for example, the observed diffracted intensity will be twice as large if the incident beam intensity is doubled where the weight of the material does not change.

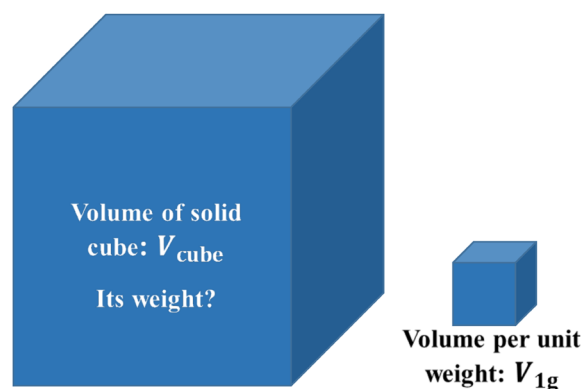


Fig. 1. Basic idea of the DDM is the same as weighing of a solid cube.

\* Senior Adviser, Rigaku Corporation.

The quantities which we would like to find in QPA are, however, relative weight ratios of the individual components. Then, under the normalization condition, the weight fraction for the  $k$ th component ( $w_k$ ) can be calculated by

$$w_k = \frac{W_k}{W_1 + W_2 + W_3 + \dots + W_K} \quad (3)$$

By substituting equation (2) into equation (3), the  $w_k$  can be given by

$$w_k = a_k S_k / \sum_{k'=1}^K a_{k'} S_{k'} \quad (4)$$

In equation (4), the proportional constant  $C$  in equation (2) is cancelled out. The scattered intensities from the individual components ( $S_k$ ) are required only in relative magnitudes. Equation (4) is used as the basic formula in the DDM, and it is called “the intensity-composition (IC) formula”. Conceptually “intensity” comes from the sum total of scattered intensities  $S_k$  and the meaning of “composition” will soon become clear.  $S_k$  in the IC formula is the observed quantity derived from the measured powder diffraction pattern. Parameter  $a_k^{-1}$  is a theoretical value whose derivation will be described in the next section.

### 3. Scattered intensity per unit weight

The parameter  $a_k^{-1}$  can be calculated by

$$a_k^{-1} = \frac{1}{M_k} \sum_{i=1}^{N_k^A} n_{ik}^2 \quad (5)$$

where  $M_k$  is the chemical formula weight of the  $k$ th component material and  $n_{ik}$  is the number of electrons belonging to the  $i$ th atoms ( $i=1-N_k^A$ ) in the chemical formula unit<sup>(10), (14)</sup>. The squared number of electron ( $n_{ik}^2$ ) represents the total scattering power of the  $i$ th atom, and the quantity  $\sum n_{ik}^2$  represent the total sum of scattered intensities from atoms in the chemical formula unit. The chemical formula weight  $M_k$  corresponds to the unit weight, and equation (5) represents the total sum of scattered intensities per unit weight. In the case, for example, of  $\alpha$ -quartz with the chemical formula of  $\text{SiO}_2$ , the chemical formula weight is given by  $M_k=28.086+2 \times 15.999=60.084$  g/mol, and the sum of the squared numbers of electrons is given by  $14^2+2 \times 8^2=324$ . Then  $a_k$  has the value of  $a_k=60.084/324=0.18544$ . The parameter  $a_k$  used in the IC formula can easily be calculated for a given chemical composition with a periodic table and a pocket calculator. Now the meaning of the “composition” in the IC formula may be clear.

Many readers of this article will wonder, “can we really calculate the total sum of scattered intensities per unit weight only from the chemical composition data?” Equation (5) was first derived by using the approximate relationship between the height and the integrated value of the peak at the origin of the Patterson function<sup>(10), (16)</sup>. Thereafter, it was theoretically verified that equation (5) holds in the case of scattered intensities from an assemblage of atoms at arbitrary positions<sup>(14)</sup>. This

means that the IC formula can be applied not only to crystalline materials but also amorphous materials.

### 4. Characteristics of the parameter $a_k^{-1}$

Atomic scattering factors and positional coordinates of individual atoms are required for calculating intensities of individual diffraction lines and theoretical powder diffraction patterns. With respect to the total sum of scattered intensities, however, it is possible to calculate it using only chemical composition data of materials with equation (5). The  $a_k^{-1}$  depends only on the chemical composition. It is an intrinsic parameter of the material, and it has the physical meaning of “the scattered intensity per unit weight”. Furthermore, it has the relationship represented by  $a_k^{-1} \approx A_k^{\text{av}}/D$ , where  $A_k^{\text{av}}$  is the average atomic weight of atoms in the chemical formula unit ( $A_k^{\text{av}}=M_k/N_k^A$ ),  $D$  is a ratio of atomic weight to atomic number, where  $D \approx 2$  ( $D=2.006$  in the case of Si). Therefore, the  $a_k^{-1}$  is proportional to the average atomic weight of the material<sup>(12), (13)</sup>.

As clearly be seen from equation (4), the parameters  $a_k$  are not needed in QPA of polymorphs with the same chemical composition. Furthermore, as will be described in Table 1, materials with similar chemical compositions have  $a_k$  values which are close to each other. As is understood from equation (5), the increase of atomic weight accompanies the increase of the number of electrons, and increases or decreases in the numerator and denominator are cancelled out. Rock forming minerals as natural products have generally complicated chemical compositions: they contain various kinds of atoms as trace elements and metal ions are replaced between the coordination polyhedra. The influence on the magnitudes of derived weight fractions is, however, negligibly small even when the ideal chemical formula is used instead of the actual chemical formula obtained by chemical analysis of natural samples. Magnitudes of errors in the derived weight fractions induced by variations in chemical compositions are discussed in reference 12.

### 5. How to derive the total sum of scattered intensities $S_k$

As was stated in §1, the observed diffraction

**Table 1.** A comparison of  $a_k$  values for series of magnesium silicate hydrates and hydrocarbons with similar chemical compositions<sup>(12)</sup>. Values at the bottom line are the averages of individual  $a_k$  values. Values in parentheses are the standard deviations for the averages.

Chemical formula	$a_k$	Chemical formula	$a_k$
$\text{Mg}_3(\text{SiO}_4)(\text{OH})_2$	0.19028	$\text{C}_{10}\text{H}_8$	0.3483
$\text{Mg}_5(\text{SiO}_4)_2(\text{OH})_2$	0.19023	$\text{C}_{14}\text{H}_{10}$	0.3468
$\text{Mg}_7(\text{SiO}_4)_3(\text{OH})_2$	0.19020	$\text{C}_{18}\text{H}_{12}$	0.3459
$\text{Mg}_9(\text{SiO}_4)_4(\text{OH})_2$	0.19019	$\text{C}_{22}\text{H}_{14}$	0.3454
Average	0.19022(4)	Average	0.3466(11)

pattern of a mixture is the superposition of individual component patterns. The corresponding calculated pattern,  $y(2\theta)$ , can be synthesized by superposing the individual component patterns, represented by  $y(2\theta)_k$ . For a  $K$ -component mixture, it is given by

$$y(2\theta) = y(2\theta)_{\text{BG}} + \sum_{k=1}^K y(2\theta)_k \quad (6)$$

where  $y(2\theta)_{\text{BG}}$  is the background intensity. The observed quantities required for the DDM are total sums of scattered intensities ( $S_k$ ) from the individual components. Therefore, it is first necessary to separate the observed pattern into the individual components  $y(2\theta)_k$ . Various techniques can be used for separating the pattern. They can be categorized into two groups. One decomposes the pattern into individual diffraction lines, and then the diffraction lines are grouped into respective components. The other one separates the pattern by directly fitting individual components  $y(2\theta)_k$  to be in proportion to relative intensity ratios.

### 5.1. Individual profile fitting technique

Individual profile fitting (IPF) technique can decompose overlapping diffraction lines present in a relatively narrow  $2\theta$ -range. It can be applied if angular positions of individual diffraction lines can be recognized. Figure 2 shows an example of applying the IPF to three overlapping diffraction lines from an  $\alpha$ -SiO<sub>2</sub>+Si mixture. The individual diffraction lines are modeled by  $I_{jk}P(2\theta)_{jk}$ , where  $I_{jk}$  is the integrated intensity parameter for the  $j$ th diffraction line of the  $k$ th component, and  $P(2\theta)_{jk}$  is the normalized profile function used for representing the profile shape<sup>(17)</sup>. The

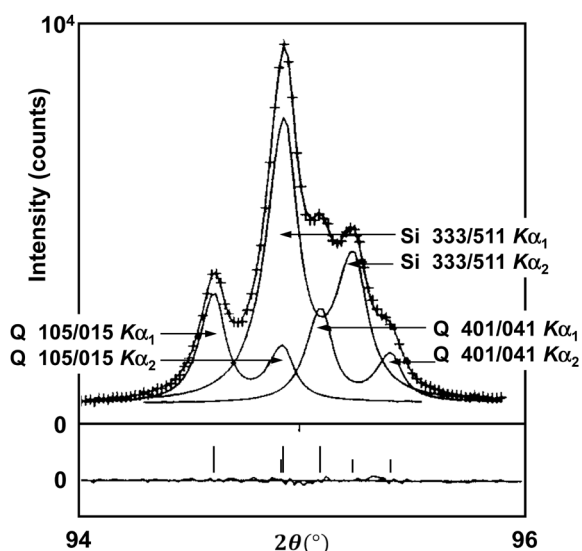


Fig. 2. Result of individual profile fitting applied to three overlapping diffraction lines from an  $\alpha$ -SiO<sub>2</sub> + Si mixture<sup>(17)</sup>. Observed and calculated intensities are represented by plus symbols and solid lines, respectively. The plot at the bottom of the diagram represents differences between the two intensities on the same scale. Short vertical bars are peak position markers.

$y(2\theta)$  can be synthesized by superposing the individual diffraction lines as shown in Fig. 2, and it can be expressed by

$$y(2\theta) = y(2\theta)_{\text{BG}} + \sum_k \sum_j I_{jk} P(2\theta)_{jk} \quad (7)$$

where  $\sum_j I_{jk} P(2\theta)_{jk}$  is identical to the  $y(2\theta)_k$  in equation (6). The  $y(2\theta)$  is least-squares fitted to the observed diffraction pattern by adjusting the integrated intensity parameters ( $I_{jk}$ ) together with peak positions, profile width and profile shape parameters. A series of least-squares fittings can automatically be conducted from the low-angle side to the high-angle side by using commercially available or freely distributed software suites. The resulting output will be a list of  $d$  values, integrated intensities ( $I$ ) and indices ( $hkl$ ) for respective phases. The  $S_k$  for each component can be obtained by summing up the  $I_{jk}$  with equation (8) (§5.2.a). Accurate datasets of  $S_k$  will be obtained with IPF technique when the observed diffraction pattern is not complicated<sup>(10),(16)</sup>.

### 5.2. Whole-powder-pattern fitting techniques

Whole-powder-pattern fitting (WPPF) techniques are powerful tools for analyzing complicated powder diffraction patterns. Currently used techniques in this category are the whole-powder-pattern decomposition (WPPD) method based on the Pawley algorithm<sup>(18)</sup> or the Le Bail algorithm<sup>(19)</sup>, the Rietveld method<sup>(7)</sup>, and the full-pattern-fitting (FPF) method<sup>(20)</sup>. This last method utilizes the single-phase observed diffraction pattern after subtracting background intensities. All of these methods have originally different analytical purposes, and they use different fitting functions for calculating the  $y(2\theta)_k$  in equation (6). In the DDM, four different types of fitting functions, with one new type in addition to the above three types, are currently available for separating diffraction patterns by WPPF. They are called type-A, B, C and C<sub>2</sub><sup>(13)-(15)</sup>, respectively. These four types of fitting functions can arbitrarily be chosen and combined in accordance with analysis conditions and then fitted simultaneously. Understanding the differences between these four functions and their applied conditions is recommended for mastering the DDM.

#### a) Type-A function: use of the WPPD method

Type-A function is the same as that used in the Pawley method for WPPD. It uses the same profile model as that used in the IPF technique [equation (7)]. All  $I_{jk}$  parameters in a wide  $2\theta$ -range are simultaneously fitted using the least-squares method. Peak positions are constrained by the unit-cell parameters, and unit-cell parameters are refined instead of the individual peak positions. After the least-squares fitting, a list of refined  $I_{jk}$  values are delivered for respective phases. The  $S_k$  can then be calculated by

$$S_k = \sum_{j=1}^{N_k} I_{jk} G_{jk} \quad (8)$$

where  $G_{jk}$  is the correction term for the Lorentz-polarization factor and the geometrical factor of the diffractometer optics<sup>(10)</sup>. Unit-cell parameters are required as input data for the phase to which the type-A function is assigned. Input of the space group, as additional information, avoids unnecessary computation and increases the accuracy in refined  $I_{jk}$  values.

#### b) Type-B function: use of pre-determined parameters of $I_{jk}$

Materials with large unit cells and low crystallographic symmetry like triclinic or monoclinic system give generally complicated diffraction patterns with many crowded peaks in the middle and high angle regions. Obtaining accurate intensity parameters becomes difficult even with a WPPD technique when the complicated diffraction patterns of two or three phases overlap. It is particularly difficult for the minor phases. In such a case, the accuracy of intensity parameters will be improved if individual  $I_{jk}$  parameters are pre-determined for respective phases. Then adjustments of scale parameters instead of the individual  $I_{jk}$  will suffice for WPPF.

$\{I'_{jk}\}$  is a dataset of integrated intensity parameters, which are pre-determined by applying the type-A function to a single-phase component material in WPPD. Type-B function uses  $Sc_k I'_{jk}$  instead of  $I_{jk}$ , where  $Sc_k$  is the scale parameter. In WPPF,  $Sc_k$  is least-squares fitted, while  $\{I'_{jk}\}$  are fixed at pre-determined values. Symbol  $I'_{jk}$  is used in order to distinguish it from the refinable parameters  $I_{jk}$  in the type-A function. When the type-B function is used, equation (8) is replaced with

$$S_k = Sc_k \sum_{j=1}^{N_k} I'_{jk} G_{jk} \quad (9)$$

Decomposing the single-phase component pattern is one of the ways to obtain  $\{I'_{jk}\}$ . The  $\{I'_{jk}\}$  can also be prepared by employing computer software for the calculation of structure factors. If a rough approximation is allowed, the  $\{I'_{jk}\}$  can be derived from the  $d$ - $I$  dataset used for the phase identification.

#### c) Type-C function: use of single-phase observed diffraction pattern after background subtraction

When the type-B function is used in WPPF, individual diffraction patterns, synthesized with the  $\{I'_{jk}\}$ , are least-squared fitted by adjusting the  $Sc_k$ . If ready-made diffraction patterns are available for the individual phases, they can be used for WPPF in place of the type-B function. A measured diffraction pattern of a single-phase component material, obtained under the same experimental conditions as those for the target mixtures, gives the ready-made diffraction pattern after subtracting the background from the pattern. The type-C function uses this background-subtracted pattern, represented by  $y(2\theta)'_k$ , in a form  $Sc_k y(2\theta)'_k$ , and it is fitted by adjusting the  $Sc_k$  in WPPF. Instead of summing up the individual  $I_{jk}$  or  $I'_{jk}$  values, the  $S_k$  can be expressed by integrating the  $Sc_k y(2\theta)'_k G(2\theta)$  over the  $2\theta$ -range  $[2\theta_L, 2\theta_H]$  used for WPPF, and it is given by

$$Y_k = Sc_k \int_{2\theta_L}^{2\theta_H} y(2\theta)'_k G(2\theta) d(2\theta) \quad (10)$$

Symbol  $Y_k$  is used instead of the  $S_k$  in the sense that the total sum of scattered intensities is the integrated value rather than the sum of discrete intensities. However, it can easily be verified that  $S_k = Y_k$ <sup>(13)</sup>. A QPA technique utilizing the observed diffraction patterns is known as the FPF method<sup>(20)</sup>. The FPF method is, however, based on the RIR method, and the RIR value must experimentally be determined with the binary mixture of the target component material and a standard reference material<sup>(13)</sup>.

When the type-A and B functions are used in WPPF, the profile models can be fitted by adjusting the parameters representing the profile width and shape together with intensity parameters  $I_{jk}$  or  $Sc_k$ . On the other hand, the type-C function, using a fixed pattern for WPPF, will induce discrepancies when the component materials are structurally unstable and change their profile widths and shapes with time. The type-C function, however, will demonstrate its power when the component pattern could neither be decomposed nor calculated based on the crystal structural model, as is often the case for low crystallinity materials.

#### d) Type-C<sub>2</sub> function: use of the single-phase observed diffraction pattern without subtracting the background

Before applying the type-C function, subtracting the background is a required step. Background subtraction is not a difficult task for patterns with well-defined background regions for the whole  $2\theta$ -range. It is, however, a difficult task when target materials are amorphous materials, low crystallinity materials like hydrates, materials with diffuse scattering due to structural defects, and many organic materials with low crystallographic symmetry that exhibit crowded weak peaks in the middle and high angle regions. The single-phase observed diffraction pattern can be represented by  $y(2\theta)^S_k = y(2\theta)'_{BG,k} + y(2\theta)'_k$ , where  $y(2\theta)'_{BG,k}$  represents the background intensity. Instead of  $Sc_k y(2\theta)'_k$  in the type-C function, the type-C<sub>2</sub> function uses  $Sc_k y(2\theta)^S_k$  without subtracting the background intensities<sup>(15)</sup>. The type-C<sub>2</sub> function can be fitted, in the same manner as the type-C function, by adjusting the  $Sc_k$ .

The  $Y_k$ , defined by equation (10), is the integrated value of peak profile intensities,  $Sc_k y(2\theta)'_k G(2\theta)$ . Quantity  $B_k$  is defined as the integrated value of background intensities,  $Sc_k y(2\theta)'_{BG,k} G(2\theta)$  in the same  $2\theta$ -range as that for the integration in equation (10). Then the quantity  $Y_k^{BP}$ , defined by  $Y_k^{BP} = B_k + Y_k$ , simply represents the integrated value of the  $Sc_k y(2\theta)^S_k G(2\theta)$  in the same  $2\theta$ -range for  $B_k$  and  $Y_k$ . WPPF will output the  $Y_k^{BP}$  for the component, to which the type-C<sub>2</sub> function is assigned. By defining the ratio  $R_k = B_k/Y_k$ , the  $Y_k^{BP}$  can be converted into the  $Y_k$  by<sup>(15)</sup>

$$Y_k = \frac{Y_k^{BP}}{1 + R_k} \quad (11)$$

The  $Y_k$  by equation (11) can be used in the IC formula.

The type- $C_2$  function can be used in combination with the other types of fitting functions. Then it is, in general, necessary to determine the ratio  $R_k$  for the component, to which the type- $C_2$  is assigned. The type- $C_2$  function can, however, be used without determining the  $R_k$  when target mixtures satisfy the following conditions,

- 1) The type- $C_2$  function is assigned to all components in a mixture.
- 2) The component materials satisfy the following condition.

$$R_1 \approx R_2 \approx R_3 \approx \dots \approx R_K \quad (12)$$

Let us consider substituting equation (11) into equation (4). The ratios  $R_k$  for all components in equation (4) are cancelled out when the condition in equation (12) holds true. In this case, the IC formula becomes

$$w_k = a_k Y_k^{\text{BP}} / \sum_{k'=1}^K a_{k'} Y_{k'}^{\text{BP}} \quad (13)$$

Therefore, we can conduct QPA with the  $Y_k^{\text{BP}}$  without subtracting the background. It is often the case that the condition in equation (12) is satisfied as in the cases of polymorphs, many organic compounds consisting of similar elements as H, C, O, N, and chemically analogous materials. For these materials, the condition  $a_1 \approx a_2 \approx a_3 \approx \dots \approx a_K$  would also hold. Real examples will be given in §7.

It should be noted that compounds containing certain elements (for example, the element Fe) exhibit high background intensities due to X-ray fluorescence emitted when  $\text{CuK}\alpha$  radiation is used for data collection. For mixtures containing compounds of this kind, equation (12) does not hold true so equation (11) must be used for that component to which the type- $C_2$  function is assigned. Two experimental techniques for determining the magnitude of  $R_k$  are described in reference 15.

## 6. Rietveld QPA and the DDM

If we reconsider the theory of QPA using the Rietveld method (Rietveld QPA), we find that the quantity corresponding to equation (5) is also calculated in Rietveld QPA<sup>(13)</sup>: the sum of scattered intensities per

unit weight is calculated by summing up the squared structure factors  $|F(hkl)|^2$  in a finite  $2\theta$ -range. This quantity will become identical to the  $a_k^{-1}$  [equation (5)] if the summation of  $|F(hkl)|^2$  is extended to infinity in reciprocal space. Rietveld QPA can be conducted with measured data in a finite  $2\theta$ -range, but crystal structure parameters are always required to calculate the  $F(hkl)$  for all components in a mixture. In QPA using the DDM, the  $a_k^{-1}$  can be calculated only from the chemical composition data, while the corresponding observed intensities should, in principle, be summed up to infinity. In practice, however, relative magnitudes of  $S_1; S_2; S_3; \dots; S_K$  are always effective in equation (4), and the  $2\theta$ -range used for WPPF are substantially the same for both Rietveld QPA and the DDM.

Four types of the fitting functions currently available in the DDM are summarized in Table 2. Rietveld QPA can be regarded as QPA using the type-B function with the intensity datasets  $\{I'_{jk}\}$  prepared by calculating  $F(hkl)$ . Individual weight fractions are derived from refined scale parameters by using the formula reported by Hill and Howard<sup>(9)</sup>. In the DDM, the observed quantities required in the IC formula are the total sums of scattered intensities ( $S_k$ ). They can be derived by using various ways as presented on the third line of Table 2. Incorporation of various types of fitting functions, as shown in Table 2, widens the applicability of the DDM to any mixtures containing highly crystalline materials to low crystallinity and amorphous materials. Even when unknown material is present in the mixture, it can be quantified by estimating its chemical composition from the batch chemical composition of the mixture<sup>(12)</sup>.

## 7. Examples of applications

Presenting real examples of applications provides a short cut for understanding how to handle the type-A to  $C_2$  functions summarized in Table 2. All examples presented below are results obtained from testing the various types of the functions used in the DDM. Mixture samples used were prepared by mixing reagent-grade chemicals weighed in specified weight ratios. Each sample was then packed, using the standard procedure, into a rotational flat specimen holder. Their profile intensities were measured by Rigaku SmartLab equipped with an X-ray source for  $\text{CuK}\alpha$  radiation and

**Table 2.** Summary of functional forms for the individual types of the subfunctions used in WPPF.

Type	A	B	C	$C_2$
$y(2\theta)_k$	$\sum_j I_{jk} P(2\theta)_{jk}$	$Sc_k \sum_j I'_{jk} P(2\theta)_{jk}$	$Sc_k y(2\theta)'_k$	$Sc_k y(2\theta)_k^S$
$S_k$	$\sum_{j=1}^{N_k} I_{jk} G_{jk}$	$Sc_k \sum_{j=1}^{N_k} I'_{jk} G_{jk}$	$Y_k$	$\frac{Y_k^{\text{BP}}}{1 + R_k}$
Adjustable intensity parameter	$I_{jk}$	$Sc_k$	$Sc_k$	$Sc_k$
Input data	Unit-cell parameters	$\{I'_{jk}\}$ , unit-cell parameters	$y(2\theta)'_k$	$y(2\theta)_k^S$

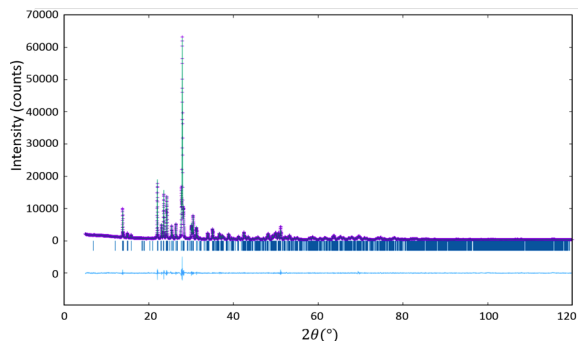


**Fig. 3.** WPPF result for the diffraction pattern of albite. Data are plotted as in Fig. 2.

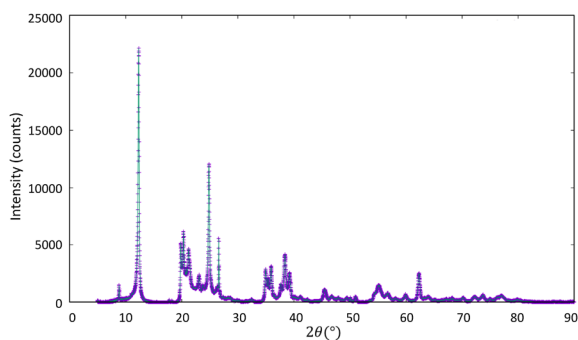


**Fig. 4.** Observed diffraction pattern of single-phase kaolinite after subtracting background intensities.

a one-dimensional silicon strip detector (D/teX Ultra 250, strip width=75 μm, 256 channels) on the diffracted beam side. Diffractometer optics were based on the Bragg-Brentano geometry, and regular dimensions were chosen for slit systems<sup>(13)-(15)</sup>. In the following,  $w_k^{\text{weigh}}$  and  $\Delta w_k$  represent the weighed value and  $\Delta w_k = w_k - w_k^{\text{weigh}}$  (in %), respectively.

**7.1. Combined use of type-A, B and C functions**

A ternary mixture consists of  $\alpha$ -quartz (SiO<sub>2</sub>), albite (NaAlSi<sub>3</sub>O<sub>8</sub>) and kaolinite (Al<sub>2</sub>Si<sub>2</sub>O<sub>5</sub>(OH)<sub>4</sub>) in weight ratios of 5 : 4 : 1, which simulate weathered granites used as raw materials in ceramics industry. Steps of QPA using the type-A, B and C functions are as follows<sup>(13)</sup>.

- 1) The Pawley-based WPPD method using the type-A function was applied to an observed diffraction pattern of single-phase albite. Least-squares refinement of intensity parameters outputs the  $\{I'_{jk}\}$ . Albite belongs to the triclinic system, and the WPPF result exhibits many crowded diffraction lines as shown in Fig. 3.
- 2) Kaolinite is a kind of clay mineral that usually exhibits broadened profiles and diffuse scattering arising from stacking disorder. Its diffraction pattern can neither be modeled without taking the structural disorder into account, nor properly decomposed with the pattern decomposition method. In Fig. 4, an observed diffraction pattern of a single phase kaolinite, after background subtraction, is shown and used as the  $\gamma(2\theta)'_k$  in the type-C function.

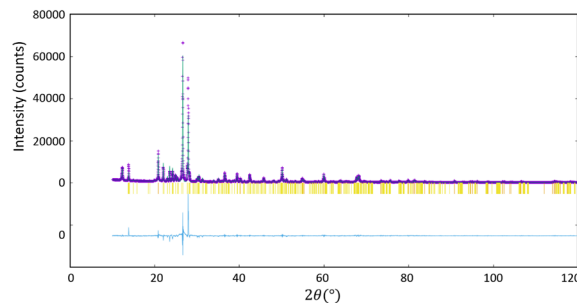


**Fig. 5.** WPPF result for the diffraction pattern of  $\alpha$ -SiO<sub>2</sub> + albite + kaolinite mixture<sup>(13)</sup>. Data are plotted as in Fig. 2.

**Table 3.** Results of QPA by the DDM for ternary mixture in three repeated scans<sup>(13)</sup>.

component	Number of Scan	$\alpha$ -quartz	albite	Kaolinite	RMSE
$w_k^{\text{weigh}}$ (%)		50.00	39.97	10.03	
$\Delta w_k$ (%)	1 <sup>st</sup>	-0.54	-0.02	0.57	0.46
	2 <sup>nd</sup>	0.78	-0.78	0.00	0.63
	3 <sup>rd</sup>	0.34	-0.81	0.47	0.57

- 3)  $\alpha$ -quartz belongs to the trigonal system with a small unit cell. Preliminary data processing was not necessary for this component material.
- 4) In QPA, the type-A, B and C functions were assigned to  $\alpha$ -quartz, albite and kaolinite, respectively. Pre-determined  $\{I'_{jk}\}$  and  $\gamma(2\theta)'_k$  in steps 1 and 2 were used in the forms of  $S_{C_k} I'_{jk}$  and  $S_{C_k} \gamma(2\theta)'_k$  for type-B (albite) and C (kaolinite) functions, respectively. In WPPF, individual  $I'_{jk}$  and two  $S_{C_k}$  parameters were refined together with the unit cell and other parameters of  $\alpha$ -quartz and albite.

Figure 5 shows the ternary mixture WPPF result. Table 3 gives results of QPA with the three intensity datasets obtained by repeated scans with the sample repacked prior to each scan. In this case, the root-mean-square error (RMSE) for  $\Delta w_k$  is  $\leq 0.6\%$ .

**7.2. QPA using type-C<sub>2</sub> function**

**a) QPA of  $\alpha$ -Al<sub>2</sub>O<sub>3</sub> +  $\gamma$ -Al<sub>2</sub>O<sub>3</sub> binary mixtures**

Samples were  $\alpha$ - and  $\gamma$ -Al<sub>2</sub>O<sub>3</sub> binary mixtures with five different weight ratios. Figure 6 shows diffraction patterns of  $\alpha$ - and  $\gamma$ -Al<sub>2</sub>O<sub>3</sub>, measured under the same experimental conditions.  $\alpha$ -Al<sub>2</sub>O<sub>3</sub> is chemically and thermally stable and is used as a standard reference material. It has high crystallinity and gives very sharp peaks as shown in Fig. 6. On the other hand,  $\gamma$ -Al<sub>2</sub>O<sub>3</sub> has the structure of a defect cubic spinel type which gives broadened profiles and diffuse scattering throughout the whole angular region. The diffraction pattern for  $\alpha$ -Al<sub>2</sub>O<sub>3</sub> can easily be modeled based on the crystal structure. On the other hand, neither pattern decomposition nor accurate determination of the background height nor structure-based modeling of diffraction pattern can realistically be applied to the

latter. In Fig. 6, profile intensities are higher for  $\gamma$ - $\text{Al}_2\text{O}_3$  than  $\alpha$ - $\text{Al}_2\text{O}_3$  in all background regions of  $\alpha$ - $\text{Al}_2\text{O}_3$ ; this is due to the diffuse scattering from  $\gamma$ - $\text{Al}_2\text{O}_3$ . Original background heights of  $\alpha$ - and  $\gamma$ - $\text{Al}_2\text{O}_3$  under the same experimental condition are, however, considered to be the same. Then it was assumed that the condition in equation (12) holds for these binary mixtures.

Observed diffraction patterns of  $\alpha$ - and  $\gamma$ - $\text{Al}_2\text{O}_3$  in Fig. 6 were used without subtracting their background intensities as  $\gamma(2\theta)_k^S$  in the type- $\text{C}_2$  function. Refined parameters were scale parameters, parameters for correcting a small shift of the pattern along the  $2\theta$ -axis ( $<0.01^\circ$  in general), and parameters in the background function. Figures 7 and 8 show WPPF results for two mixtures with weight ratios of 95:5 and 5:95. Table 4 gives QPA results. Average value of  $|\Delta w_k|$  for five mixtures ( $|\Delta w_{k|\text{lav}}$ ) is just 0.05%. In Fig. 7, it was hard to see a trace of  $\gamma$ - $\text{Al}_2\text{O}_3$  pattern; nevertheless  $\gamma$ - $\text{Al}_2\text{O}_3$  was accurately quantified.

**b) QPA of amorphous component**

Samples were binary mixtures of  $\alpha$ -quartz ( $\text{SiO}_2$ ) and glass- $\text{SiO}_2$  in four different weight ratios. As in the same manner as the previous example, the diffraction pattern of single-phase  $\alpha$ -quartz and the halo pattern of glass- $\text{SiO}_2$  were separately measured, and both patterns were used with the type- $\text{C}_2$  function without subtracting their background intensities. Figure 9 shows a WPPF result and Table 5 gives QPA results.

In QPA of mixtures containing an amorphous component, the type-C function can be assigned to the amorphous halo after subtracting the background intensities. However, whole profile of the amorphous

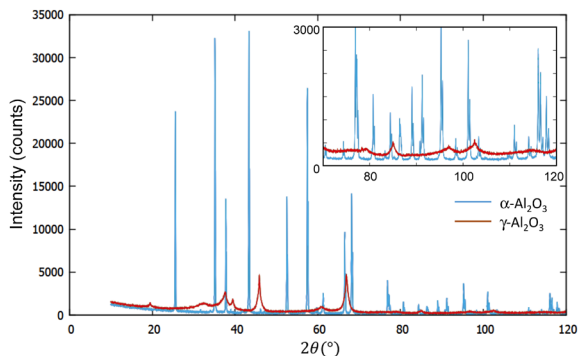


**Fig. 6.** Observed diffraction patterns of single phase  $\alpha$ - and  $\gamma$ - $\text{Al}_2\text{O}_3$  powders measured under the same experimental condition superimposed on the same intensity scale. Inset image represents part of the diagram with an enlarged scale.

**Table 4.**  $w_k^{\text{weigh}}$  and  $\Delta w_k$  (in %) for  $\alpha$ - and  $\gamma$ - $\text{Al}_2\text{O}_3$  mixtures with five different weight ratios. Data are given only for  $\gamma$ - $\text{Al}_2\text{O}_3$  since those for  $\alpha$ - $\text{Al}_2\text{O}_3$  can be obtained by  $1 - w_k^{\text{weigh}}$  and  $-\Delta w_k^{(15)}$ .

wt. ratio	95:5	75:25	50:50	25:75	5:95	$ \Delta w_{k \text{lav}}$
$w_k^{\text{weigh}}(\%)$	5.01	25.05	50.04	75.00	95.01	
$\Delta w_k(\%)$	-0.04	-0.10	-0.00	-0.05	-0.06	0.05

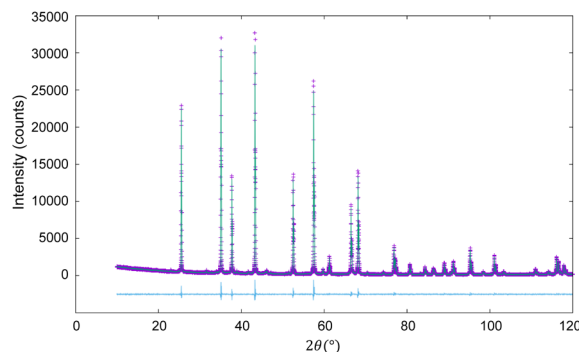


**Fig. 7.** WPPF result for the diffraction pattern of  $\alpha$ - and  $\gamma$ - $\text{Al}_2\text{O}_3$  mixture with a weight ratio of 95:5<sup>(15)</sup>. Data are plotted as in Fig. 2.

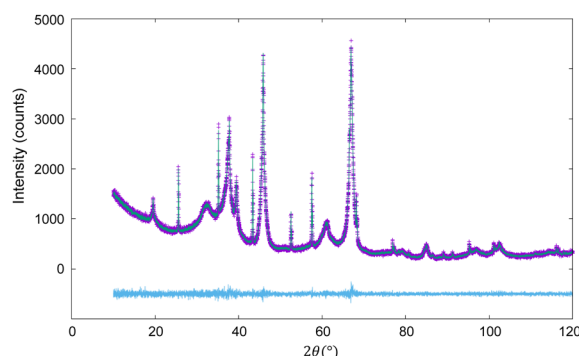


**Fig. 8.** WPPF result for the diffraction pattern of  $\alpha$ - and  $\gamma$ - $\text{Al}_2\text{O}_3$  mixture with a weight ratio of 5:95<sup>(15)</sup>. Data are plotted as in Fig. 2.

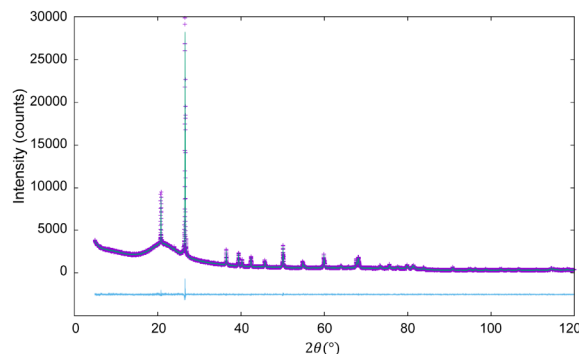


**Fig. 9.** WPPF result for the diffraction pattern of  $\alpha$ -quartz ( $\text{SiO}_2$ ) and  $\text{SiO}_2$  glass mixture in a weight ratio of 2:8<sup>(15)</sup>. Data are plotted as in Fig. 2.

**Table 5.**  $w_k^{\text{weigh}}$  and  $\Delta w_k$  (in %) for  $\alpha$ -quartz ( $\text{SiO}_2$ ) and  $\text{SiO}_2$  glass mixtures with four different weight ratios. Data are given only for glass components.  $|\Delta w_{k|\text{lav}}$  represents the average of four  $|\Delta w_k|^{(15)}$ .

wt. ratio	80:20	60:40	40:60	20:80	$ \Delta w_{k \text{lav}}$
$w_k^{\text{weigh}}(\%)$	19.68	40.35	60.01	80.17	
$\Delta w_k(\%)$	0.4	-0.2	-0.4	-0.7	0.4

halo interferes with the background function inducing a large error in QPA<sup>(14)</sup>. The type-C<sub>2</sub> function can avoid this interaction with the background function, so that it derives accurate QPA results as shown in Table 5<sup>(15)</sup>.

## 8. Summary

Basic principles and operation methods of the DDM have been described. The DDM is based on a simple principle, the basic idea of which is expressed by equation (1). Observed quantities, required for conducting the DDM, are the total sums of scattered intensities from individual component phases, while the scattered intensity per unit weight can be calculated only from the chemical composition data. WPPF technique is a powerful tool for separating the observed diffraction pattern into individual component patterns. Four fitting functions of different types can arbitrarily be chosen, combined and fitted simultaneously. The type-C<sub>2</sub> function is a recent addition to powder diffraction data analysis. A few parameters were least-squares fitted in the WPPF technique, with the least-squares refinement being very fast and stable. Any scientist should be able to routinely derive the same quality QPA results using the type-C<sub>2</sub> function. The simplicity of the type-C<sub>2</sub> function within WPPF is considered to be best suited for QPA in the quality control of industrial products<sup>(15)</sup>.

In modern crystal structure analysis, concern is focused on fine structures revealing deviations from the average structure. Examples are nano crystals, disordered crystals, amorphous materials *etc.* In QPA, demands for the quantification of more complex

mixtures, in which component materials in various crystalline states coexist, are expected increase in the future. Developing the DDM was a response to these demands. Development of additional techniques for pattern separation is also expected to continue.

## References

- (1) H. P. Klug and L. E. Alexander: *X-ray Diffraction Procedure for Polycrystalline and Amorphous Materials*, Wiley, (1974).
- (2) H. Toraya, M. Yoshimura and S. Somiya: *J. Am. Ceram. Soc.*, **67** (1984), C199–C121.
- (3) D. Y. Li, B. H. O'Connor, Q. T. Chen and M. G. Zadnik: *J. Am. Ceram. Soc.*, **77** (1994), 2195–2198.
- (4) L. E. Alexander and H. P. Klug: *Anal. Chem.*, **20** (1948), 886–889.
- (5) F. H. Chung: *J. Appl. Cryst.*, **7** (1974), 519–525.
- (6) F. H. Chung: *J. Appl. Cryst.*, **7** (1974), 526–531.
- (7) H. M. Rietveld: *J. Appl. Cryst.*, **2** (1969), 65–71.
- (8) P.-E. Werner, S. Salome and G. Malmros: *J. Appl. Cryst.*, **12** (1979), 107–109.
- (9) R. J. Hill and C. J. Howard: *J. Appl. Cryst.*, **20** (1987), 467–474.
- (10) H. Toraya: *J. Appl. Cryst.*, **49** (2016), 1508–1516.
- (11) H. Toraya: *J. Appl. Cryst.*, **50** (2017), 665.
- (12) H. Toraya: *J. Appl. Cryst.*, **50** (2017), 820–829.
- (13) H. Toraya: *J. Appl. Cryst.*, **51** (2018), 446–455.
- (14) H. Toraya and K. Omote: *J. Appl. Cryst.*, **52** (2019), 13–22.
- (15) H. Toraya: *J. Appl. Cryst.*, **52** (2019), 520–531.
- (16) H. Toraya: *Rigaku J.*, **34**, (2018), 3–8.
- (17) R. A. Young (Ed.): *The Rietveld Method*, Oxford Univ. Press, (1995).
- (18) G. S. Pawley: *J. Appl. Cryst.*, **14** (1981), 357–361.
- (19) A. Le Bail, H. Duroy and J. L. Fourquet: *Mater. Res. Bull.* **23** (1988), 447–452.
- (20) D. K. Smith, G. G. Johnson Jr, A. Scheible, A. M. Wims, J. L. Johnson and G. Ullmann: *Powder Diffr.* **2** (1987), 73–77.